JOC Article

A Hydrogen-Bonding-Modulated Molecular Rotor: Environmental Effect in the Conformational Stability of Peptidomimetic Macrocyclic Cyclophanes

Ignacio Alfonso, M. Isabel Burguete, and Santiago V. Luis*

Departamento de Química Inorgánica y Orgánica, UAMOA, Universidad Jaume I, Campus del Riu Sec, Avenida Sos Baynat, s/n, E-12071 Castellón, Spain

luiss@qio.uji.es

Received September 21, 2005

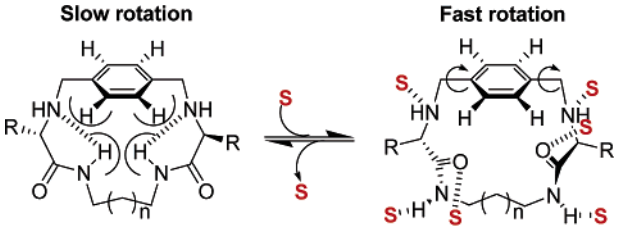

The conformational behavior of 16- to 18-membered ring peptidomimetic *p*-cyclophanes **1a,b**−**3a,b** has been studied by NMR. The cycles bearing 16 and 17 atoms showed a dynamic process within the NMR time scale, produced by the rotation of the aromatic *p*-diphenylene moiety with respect to the macrocyclic main plane. The temperature dependence of ^{1}H NMR spectra has been studied in order to get activation parameters of the energetic barrier for the process (VT-NMR and line shape analysis). The rate of the movement clearly depends on the macrocyclic ring size and the nature of the peptidomimetic side chain. Entropic and enthalpic contributions to the free energy of activation are discussed. The rotation of the aromatic ring is closely related to the intramolecular hydrogen bonding pattern, as suggested by temperature factors of N*H* chemical shifts ($\Delta\delta$N*H*/ΔT) and molecular modeling. The interconnected roles of the solvation and the intramolecular H-bonds have been established by measurements (VT-NMR and $\Delta\delta$N*H*/ΔT) in environments of different polarities and H-bonding abilities. We concluded that the conformational stability of the systems directly depends on the stability of the intramolecular H-bonding pattern. We finally showed how one of these peptidomimetics behaves as a methanol-dependent artificial molecular rotor. In this simple molecular device, the well-defined molecular rotation is tuned by the competition between intramolecular hydrogen bonds and interactions with the solvent.

Introduction

Macrocyclic peptidomimetic cyclophanes are very interesting compounds in synthetic,[1] bioorganic,[2] medicinal,[3] and supramolecular chemistry.[4] Their applications range from biomedical purposes to materials science. Their cyclic structure usually confers them a well-defined three-dimensional disposition of the amino acid residues in a preferred conformation.[5] Moreover, their macrocyclic structures allow them to host small molecules and ions,[6] with an interesting potential in the molecular recognition field and in the design of new chemosensors.[7] Finally, the availability of both enantiomers of different amino acids with varied functionalities on the side chains make them very versatile building blocks for the synthesis of more complex structures in order to achieve compounds with desired properties.[8]

* To whom correspondence should be addressed. Ph: +34 964728239. Fax: +34 964728214.

(1) (a) Billing, J. F.; Nilsson, U. J. *J. Org. Chem.* **2005**, *70*, 4847−4850. (b) Punna, S.; Kuzelka, J.; Wang, Q.; Finn, M. G. *Angew. Chem., Int. Ed.* **2005**, *44*, 2215−2220. (c) Cristau, P.; Martin, M.-T.; Tran Hu Dau, M.-E.; Vors, J.-P.; Zhu, J. *Org. Lett.* **2004**, *6*, 3183−3186. (d) Redman, J. E.; Wilcoxen, K. M.; Ghadiri, M. R. *J. Comb. Chem.* **2003**, *5*, 33−40. (e) Locardi, E.; Stöckle, M.; Garner, S.; Kessler, H. *J. Am. Chem. Soc.* **2001**, *123*, 8189−8196. (f) Dietrich, B.; Viout, P.; Lehn, J.-M. *Macrocyclic Chemistry*; VCH: New York, 1993. (g) Parker, D. *Macrocycle Synthesis: A Practical Approach*; Oxford University Press: New York, 1996. (h) Vögtle, F. *Cyclophane Chemistry*; Wiley: Chichester, 1993.

10.1021/jo051974i CCC: $33.50
Published on Web 02/10/2006

Probably one of the most important topics when studying these molecules is their structure in solution, because very often their activity or molecular properties strongly depend on that. Factors such as H-bonding pattern, size of the macrocyclic cavity, polarity, conformational preferences, or rigidity are crucial for understanding the behavior of this family of compounds. Nuclear magnetic resonance (NMR) and molecular modeling are probably some of the most powerful tools for getting information about structures in solution.[9] Here we report on the structural analysis of peptidomimetic cyclophanes **1a,b**−**3a,b** (Chart 1), stressing the dynamic behavior of the aromatic moiety. The effects of macrocyclic ring size, temperature, side chains, and solvent polarity are deeply screened. The microscopic understanding of these processes would be critical for the design of new molecular devices.[10] On the other hand, these systems are very simple models for studying conformational flexibility and stability, in a deep relationship with solvent exclusion[11] and, therefore, with protein folding processes.[12]

CHART 1. Molecular Structures of the Peptidomimetic Cyclophanes 1a,b−3a,b Studied in This Work

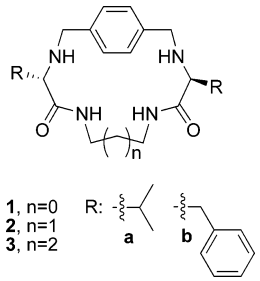

Results and Discussion

Conformational Flexibility in Solution. In a previous paper, we described the syntheses of several peptidomimetic macrocycles **1a,b**−**3a,b** through a high yield macrocyclization step, with no need of protecting groups or high dilution techniques.[13] The efficiency of the process was explained by a preorganization of the peptidomimetic precursors, due to a combination of intramolecular H-bonding and solvophobic effects. When analyzing the NMR data of the final compounds, an intriguing pattern was observed depending on the length of the aliphatic moiety. Thus, for instance, in the ^{1}H NMR spectra, the spin system for the aromatic signals of the *p*-diphenylene substructure (ArH) changed from AA′BB′ to A_2 as the length of the aliphatic spacer increased (see Figure 1). Accordingly, for the same aromatic part, the number of ^{13}C NMR signals also decreased from three (two methynes and one quaternary carbon) to two (only one CH signal and the mentioned quaternary C) when enlarging the size of the cyclic compounds.[13] A plausible explanation for this effect arose from a restricted rotation of the aromatic ring with respect to the macrocyclic main plane (Scheme 1). Actually, the solid-state structure of **1a** presented the aromatic moiety perpendicular to the peptidomimetic arm,[13] an arrangement that could be the ground state of the proposed conformational movement. Considering the C_2 symmetry of the compounds, the spin system of the *p*-diphenylene moiety should be AA′BB′ in the slow movement regime but A_2 when this rotation is fast in the NMR time scale. As for the rotation of the aromatic ring, this has to pass one −CH═CH− fragment through the inner cavity of the macrocycle, and the larger is the size of the cavity, the easier is the fast rotation of the diphenylene moiety. This assumption would explain the observed differences in the NMR spectra, which encouraged us to study this conformational equilibrium in detail. Besides, this

(2) (a) Horne, W. S.; Stout, C. D.; Ghadiri, M. R. *J. Am. Chem. Soc.* **2003**, *125*, 9372−9376. (b) Fernández-López, S.; Kim, H.-S.; Choi, E. C.; Delgado, M.; Granja, J. R.; Khasanov, A.; Kraehenbuehl, K.; Long, G.; Weinberger, D. A.; Wilcoxen, K. M.; Ghadiri, M. R. *Nature* **2001**, *412*, 452−455.

(3) (a) Loughlin, W. A.; Tyndall, J. D. A.; Glenn, M. P.; Fairlie, D. P. *Chem. Rev.* **2004**, *104*, 6085−6117. (b) Reid, R. C.; Abbenante, G.; Taylor, S. M.; Fairlie, D. P. *J. Org. Chem.* **2003**, *68*, 4464−4471. (c) Reid, R. C.; Pattenden, L. K.; Tyndall, J. D. A.; Martin, J. L.; Walsh, T.; Fairlie, D. P. *J. Med. Chem.* **2004**, *47*, 1641−1651. (d) Hu, X.; Nguyen, K. T.; Verlinde, C. L. M. J.; Hol, W. G. J.; Pei, D. *J. Med. Chem.* **2003**, *46*, 3771−3774. (e) Glenn, M. P.; Pattenden, L. K.; Reid, R. C.; Tyssen, D. P.; Tyndall, J. D. A.; Birch, C. J.; Fairlie, D. P. *J. Med. Chem.* **2002**, *45*, 371−381.

(4) For some examples of related systems, see: (a) Choi, K.; Hamilton, A. D. *Coord. Chem. Rev.* **2003**, *240*, 101−110. (b) Choi, K.; Hamilton, A. D. *J. Am. Chem. Soc.* **2003**, *125*, 10241−10249. (c) Choi, K.; Hamilton, A. D. *J. Am. Chem. Soc.* **2001**, *123*, 2456−2457. (d) Somogyi, L.; Haberhauer, G.; Rebek, J., Jr. *Tetrahedron* **2001**, *57*, 1699−1708. (e) Conn, M. M.; Rebek, J., Jr. *Chem. Rev.* **1997**, *97*, 1647−1668.

(5) (a) Reyes, S. J.; Burgess, K. *Tetrahedron: Asymmetry* **2005**, *16*, 1061−1069. (b) Singh, Y.; Stoermer, M. J.; Lucke, A. J.; Guthrie, T.; Fairlie, D. P. *J. Am. Chem. Soc.* **2005**, *127*, 6563−6572. (c) Velasco-Torrijos, T.; Murphy, P. V. *Org. Lett.* **2004**, *6*, 3961−3964. (d) Mann, E.; Kessler, H. *Org. Lett.* **2003**, *5*, 4567−4570. (e) Singh, Y.; Stoermer, M. J.; Lucke, A. J.; Glenn, M. P.; Fairlie, D. P. *Org. Lett.* **2002**, *4*, 3367−3370. (f) Sastry, T. V. R. S.; Banerji, B.; Kumar, S. K.; Kunwar, A. C.; Das, J.; Nandy, J. P.; Iqbal, J. *Tetrahedron Lett.* **2002**, *43*, 7621−7625. (g) Reid, R. C.; Kelso, M. J.; Scanlon, M. J.; Fairlie, D. P. *J. Am. Chem. Soc.* **2002**, *124*, 5673−5683.

(6) (a) Heinrichs, G.; Kubic, S.; Lacour, J.; Vial, L. *J. Org. Chem.* **2005**, *70*, 4498−4501 (b) Otto, S.; Kubik, S. *J. Am. Chem. Soc.* **2003**, *125*, 7804−7805. (c) Heinrichs, G.; Vial, L.; Lacour, J.; Kubic, S. *Chem. Commun.* **2003**, 1252−1253. (d) Kubic, S.; Kirchner, R.; Nolting, D.; Seidel, J. *J. Am. Chem. Soc.* **2002**, *124*, 12752−12760. (e) Bitta, J.; Kubik, S. *Org. Lett.* **2001**, *3*, 2637−2640. (f) Kubik, S.; Goddard, R.; Kirchner, R.; Nolting, D.; Seidel, J. *Angew. Chem., Int. Ed.* **2001**, *40*, 2648−2651. (g) Pohl, S.; Goddard, R.; Kubik, S. *Tetrahedron Lett.* **2001**, *42*, 7555−7558. (h) Ishida, H.; Inoue, Y. *Biopolymers* **2000**, *55*, 469−478.

(7) (a) Galindo, F.; Becerril, J.; Burguete, M. I.; Luis, S. V.; Vigara, L. *Tetrahedron Lett.* **2004**, *45*, 1659−1662. (b) Galindo, F.; Burguete, M. I.; Luis, S. V. *Chem. Phys.* **2004**, *302*, 287−294. (c) Becerril, J.; Burguete, M. I.; Escuder, B.; Galindo, F.; Gavara, R.; Miravet, J. F.; Luis, S. V.; Peris, G. *Chem. Eur. J.* **2004**, *10*, 3879−3890. (d) Galindo, F.; Burguete, M. I.; Vigara, L.; Luis, S. V.; Russell, D. A.; Kabir, N.; Gavrilovic, J. *Angew. Chem., Int. Ed.* **2005**, *44*, 6504−6508.

(8) Copola, G. M.; Shuster, H. F. *Asymmetric Synthesis. Costruction of Chiral Molecules using Amino Acids*; Wiley: New York, 1987.

(9) See for instance: (a) Takeuchi, Y.; Marchand, A. P. *Applications of NMR Spectroscopy to Problems in Stereochemistry and Conformational Analysis*; VCH: Weinheim, 1986. (b) Ernst, L. *Prog. Nucl. Magn. Reson. Spectrosc.* **2000**, *37*, 47−190. (c) Salvatella, X.; Giralt, E. *Chem. Soc. Rev.* **2003**, *32*, 365−372. For some recent specific examples, see: (d) Xiao, J.; Weisblum, B.; Wipf, P. *J. Am. Chem. Soc.* **2005**, *127*, 5742−5743. (e) Baker, M. V.; Bosnich, M. J.; Brown, D. H.; Byrne, L. T.; Hesler, V.; Skelton, B. W.; White, A. H.; Williams, C. C. *J. Org. Chem.* **2004**, *69*, 7640−7652. (f) Peter, C.; Rueping, M.; Wörner, H. J.; Jaun, B.; Seebach, D.; van Gunsteren, W. F. *Chem. Eur. J.* **2003**, *9*, 5838−5849. (g) Cárdenas, F.; Caba, J. M.; Feliz, M.; Lloyd-Williams, P.; Giralt, E. *J. Org. Chem.* **2003**, *68*, 9554−9562. (h) Tabudravu, J. N.; Jaspar, M.; Morris, L. A.; Kettenes-van den Bosch, J. J.; Smith, N. *J. Org. Chem.* **2002**, *67*, 8593−8601.

(10) For some recent revisions, see: (a) Kottas, G. S.; Clark, L. I.; Horinek, D.; Michl, J. *Chem. Rev.* **2005**, *105*, 1281−1376. (b) Sauvage, J.-P. *Chem. Commun.* **2005**, 1507−1510. (c) Mandl, C. P.; König, B. *Angew. Chem., Int. Ed.* **2004**, *43*, 1622−1624. (d) Jimenez-Molero, M. C.; Dietrich-Buchecker, C.; Sauvage, J.-P. *Chem. Commun.* **2003**, 1613−1616. (e) Balzani, V.; Credi, A.; Venturi, M. *Chem. Eur. J.* **2002**, *8*, 5525−5530. (f) Balzani, V.; Credi, A.; Raymo, F. M.; Stoddart, J. F. *Angew. Chem., Int. Ed.* **2000**, *39*, 3348−3391.

(11) Jusuf, S.; Axelsen, P. H. *Biochemistry* **2004**, *43*, 15446−15452 and references therein.

(12) (a) Gray, R.; Trent, J. O. *Biochemistry* **2005**, *44*, 2469−2477. (b) Jourdan, M.; Searle, M. S. *Biochemistry* **2001**, *40*, 10317−10325.

(13) Becerril, J.; Bolte, M.; Burguete, M. I.; Galindo, F.; García-España, E.; Luis, S. V.; Miravet, J. F. *J. Am. Chem. Soc.* **2003**, *125*, 6677−6686.

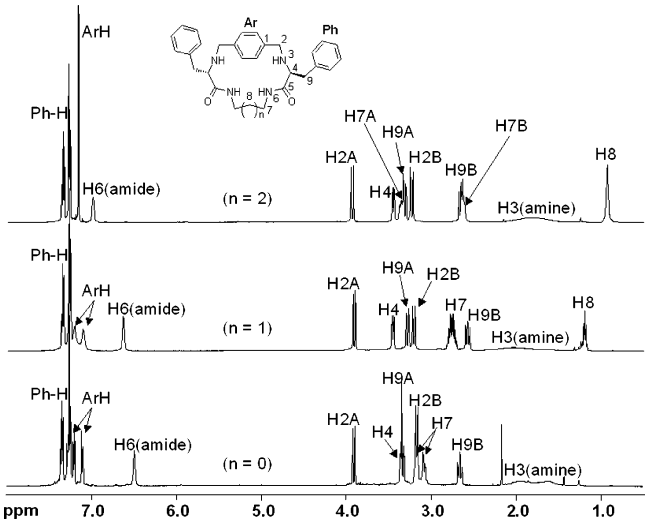

FIGURE 1. ^{1}H NMR spectra of compounds **1b**−**3b** (500 MHz, $CDCl_3$, 303 K). Assignation of the signals (by means of COSY experiments) and assumed atom numbering are also shown.

SCHEME 1. Proposed Conformational Equilibrium of Peptidomimetic Cyclophanes

is in agreement with conformational studies on simple polyazacyclophanes that showed a related behavior.[14]

Variable Temperature Nuclear Magnetic Resonance (VT-NMR) Study. Considering the proposed conformational equilibria, we decided to study the temperature dependence of the ^{1}H NMR spectra of **1a,b**−**3a,b**.[15] Different solvents were needed for covering the very different temperature ranges involved. The aromatic signals of the *p*-diphenylene moiety showed an AA′BB′ spin system at low temperature for **1a,b** and **2a,b**, reaching coalescence as the temperature was increased and giving rise to a singlet (A_2 spin system) at high temperature. Partial NMR spectra for **1a** and **2b** at different temperatures are shown in Figures 2 and 3, respectively (see also Supporting Information). Coalescence temperatures (T_c) are given in Table 1, as well as the free energies of activation ($\Delta G^{\ddagger}$) at the coalescence temperature.[16] It was impossible to observe decoalescence of the signals for the larger cycles **3a,b** within our accessible temperature range, suggesting a rotational barrier lower than 9.3 kcal/mol.

By comparing the values in Table 1, very interesting trends were obtained. The enlargement of the cyclic structure by one methylene decreases the conformational energy barrier ca. 5 kcal/mol, which is in agreement with reported data on polyamino cyclophanes.[14] Apart from the higher conformational rigidity

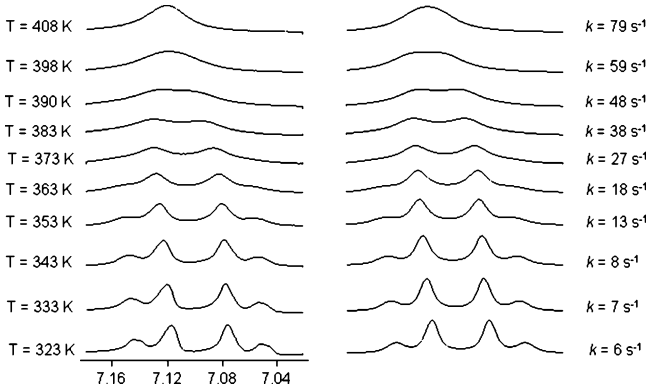

FIGURE 2. Aromatic *p*-diphenylene region of the experimental (left) and simulated (right) VT-NMR spectra of **1a** (5 mM, DMSO-d_6, 300 MHz). Values of temperature (T, K) and interconversion rate (k, s^{-1}) are also given for every trace. Simulated spectra were obtained with the gNMR program.[17]

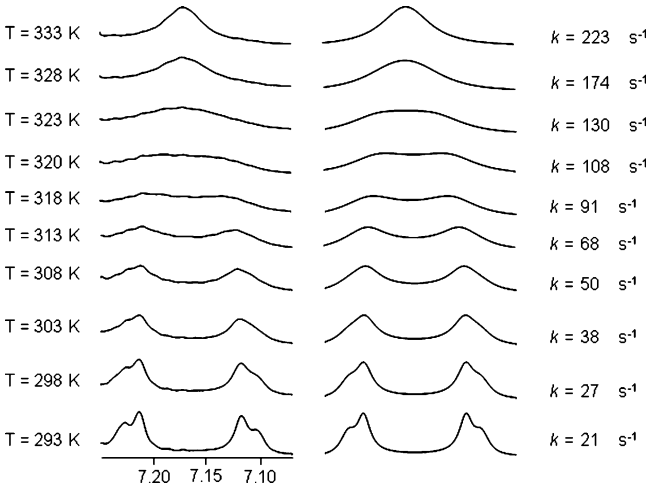

FIGURE 3. Aromatic *p*-diphenylene region of the experimental (left) and simulated (right) VT-NMR spectra of **2b** (5 mM, $CDCl_3$, 500 MHz). Values of temperature (T, K) and interconversion rate (k, s^{-1}) are also given for every trace. Simulated spectra were obtained with the gNMR program.[17]

(14) (a) Burguete, M. I.; Escuder, B.; García-España, E.; López, L.; Luis, S. V.; Miravet, J. F.; Querol, M. *Tetrahedron Lett*. **2002**, *43*, 1817−1819. (b) Burguete, M. I.; Escuder, B.; García-España, E.; Luis, S. V.; Miravet, J. F. *Tetrahedron* **2002**, *58*, 2839−2846. (c) Burguete, M. I.; Escuder, B.; García-España, E.; Luis, S. V.; Miravet, J. F. *J. Org. Chem.* **1994**, *59*, 1067−1071.

(15) For very recent examples on dynamic NMR applied to conformational analysis, see: (a) Dalla Cort, A.; Gasparrini, F.; Lunazzi, L.; Mandolini, L.; Mazzanti, A.; Pasquini, C.; Pierini, M.; Rompietti, R.; Schiaffino, L. *J. Org. Chem.* **2005**, *70*, 8877−8883. (b) Casarini, D.; Coluccini, C.; Lunazzi, L.; Mazzanti, A. *J. Org. Chem.* **2005**, *70*, 5098−5102. (c) Lunazzi, L.; Mazzanti, A.; Minzoni, M.; Anderson, J. E. *Org. Lett.* **2005**, *7*, 1291−1294. (d) González-Núñez, M. E.; Mello, R.; Royo, J.; Asensio, G.; Monzó, I.; Tomás, F.; García-López, J.; López-Ortiz, F. *J. Org. Chem.* **2005**, *70*, 3450−3457. (e) Lam, P. C.-H.; Carlier, P. R. *J. Org. Chem.* **2005**, *70*, 1530−1538. (f) Lunazzi, L.; Mazzanti, A.; Mizoni, M. *J. Org. Chem.* **2005**, *70*, 456−462. (g) Qadir, M.; Cobb, J.; Sheldrake, P. W.; Whittall, N.; White, A. J. P.; Hii, K. K.; Horton, P.; Hursthouse, M. B. *J. Org. Chem.* **2005**, *70*, 1545−1551. (h) Qadir, M.; Cobb, J.; Sheldrake, P. W.; Whittall, N.; White, A. J. P.; Hii, K. K.; Horton, P.; Hursthouse, M. B. *J. Org. Chem.* **2005**, *70*, 1551−1557. (i) Viñas, C.; Llop, J.; Teixidor, F.; Kivekäs, R.; Sillanpä, R. *Chem. Eur. J.* **2005**, *11*, 1933−1941. (j) Casarini, D.; Lunazzi, L.; Mazzanti, A.; Mercandelli, P.; Sironi, A. *J. Org. Chem.* **2004**, *69*, 3574−3577. (k) Casarini, D.; Coluccini, C.; Lunazzi, L.; Mazzanti, A.; Rompietti, R. *J. Org. Chem.* **2004**, *69*, 5746−5748. (l) Bartoli, G.; Lunazzi, L.; Massaccesi, M.; Mazzanti, A. *J. Org. Chem.* **2004**, *69*, 821−825. (m) Alezra, V.; Bernardinelli, G.; Corminboeuf, C.; Frey, U.; Kündig, E. P.; Merbach, A. E.; Saudan, C. M.; Viton, F.; Weber, J. *J. Am. Chem. Soc.* **2004**, *126*, 4843−4853. (n) Grilli, S.; Lunazzi, L.; Mazzanti, A.; Pinamonti, M. *Tetrahedron* **2004**, *60*, 4451−4458. (o) Rashkin, M. J.; Hughes, R. M.; Calloway, N. T.; Waters, M. L. *J. Am. Chem. Soc.* **2004**, *126*, 13320−13325.

(16) Sandström, J. *Dynamic NMR Spectroscopy*; Academic: London, 1982.

TABLE 1. Data from VT-NMR Experiments on 1a,b−3a,b

entry	compound	$\delta\nu^a$	T_c (K)	$\Delta G^{\ddagger}_c$ (kcal/mol)^{b,c}	solvent
1	**1a**	17.3	390	20.2	DMSO-d_6
2	**2a**	62.8	299	14.6	$CDCl_3$
3	**3a**	*d*	<200	<9.3[e]	CD_2Cl_2
4	**1b**	27.7	>413	>21.1[e]	DMSO-d_6
5	**2b**	54.0	320	15.8	$CDCl_3$
6	**3b**	*d*	<200	<9.3[e]	CD_2Cl_2

[a] Measured at the low-temperature spectra. [b] Calculated using the approximated formula for temperature of coalescence and considering the coupling constant between interconverting protons (J_{AB}). [c] Estimated error ±0.4 kcal/mol. [d] Decoalescence/coalescence not completely observed. [e] Estimated.

TABLE 2. Activation Parameters (±0.15 kcal/mol) for Compounds 1a,b−2a,b

entry	compound	E_a kcal/mol	$\Delta H^{\ddagger}$ kcal/mol	$\Delta S^{\ddagger}$ cal/K/mol	$\Delta G^{\ddagger}_{(298)}$ kcal/mol	solvent
1	**1a**	9.7	6.5	−33.6	16.5	DMSO-d_6
2	**2a**	10.8	10.2	−14.4	14.5	$CDCl_3$
3	**1b**	7.2	6.5	−36.1	17.2	DMSO-d_6
4	**2b**	11.9	11.4	−14.3	15.7	$CDCl_3$

of the smaller cycles, an unexpected effect of the side chain nature is also noteworthy. Thus, comparing entries 1 vs 4 and 2 vs 5, we can conclude that the phenylalanine derivatives lead to less flexible cycles, at least regarding the ring inversion process. This energy barrier difference is on the same range (1 kcal/mol) in all the tested examples. The smooth energy gap obtained when changing ^{i}Pr into Bn could come either by a higher stability of the conformation in the ground state (GS) and/or a lower stability of the corresponding transition states (TS). To try to clarify this topic, the activation parameters of **1a,b** and **2a,b** were calculated by performing the line shape analysis of the spectra at different temperatures (Figures 2 and 3 for **1a** and **2b**, the rest given in Supporting Information). Besides, this analysis will allow us to know the temperature dependence of the conformational energy barrier itself. Arrhenius activation energies (E_a) or enthalpic ($\Delta H^{\ddagger}$) and entropic ($\Delta S^{\ddagger}$) contributions to the free energy of activation were obtained either by ln(k) vs 1/T or Eyring plots, respectively (Table 2).[16]

The most interesting feature from values of Table 2 is the strong temperature dependence of the free energy of activation for this conformational process.[18] Thus, the value of the entropy of activation is negative in all the cases. Besides, $\Delta S^{\ddagger}$ is larger for the smaller cycles, being predominant over $\Delta H^{\ddagger}$ in its contribution to $\Delta G^{\ddagger}$. As entropy can be seen as the thermodynamic measurement of molecular disorder, the negative value of $\Delta S^{\ddagger}$ should mean that the TS has to be more ordered than the GS. This molecular order could come from a less flexible TS, having a lower number of degrees of freedom than the GS and thus leading to a molecular constriction and to a negative $\Delta S^{\ddagger}$. Obviously, this effect would be more important for the smallest cycles **1a,b**, as they are expected to show more strained TS. Another possibility for the negative entropy of activation would be a more solvated TS compared to the stable GS: the increase of solvation would order more molecules of solvent around the macrocycle, and thus $\Delta S^{\ddagger}$ should be negative. Interestingly, the effect of the side chains is entropic in the case of the 16-membered rings (see entries 1 and 3 in Table 2), whereas for the 17-membered rings, this energetic difference is enthalpic (entries 2 and 4 in Table 2). As by comparing rings of the same size, the change in the internal molecular order from GS to TS should be very similar, the entropic difference between **1a** and **1b** is most likely related to the solvation properties of both. Regarding **2a** and **2b**, there is a clear difference in stability (enthalpic contribution), which has to come from different interactions in the GS or in the TS. These results must be carefully considered as the measurements have been performed in very different solvents for the smaller and larger macrocycles. In these peptidomimetic systems, factors such as hydrogen bonding could play a very important role in the conformational preferences and have to be taken into account.

TABLE 3. Temperature Factors of N*H* Chemical Shifts for 1a,b and 2a,b

entry	compound	$\Delta\delta$N$H/\Delta T$ (ppb/K)	solvent
1	**1a**	−3.61	DMSO-d_6
2	**2a**	−2.18	$CDCl_3$
3	**1b**	−3.51	DMSO-d_6
4	**2b**	−1.91	$CDCl_3$

Hydrogen Bonding Pattern. Because of the differences observed in the previous section, we decided to study the hydrogen bonding pattern for those compounds. As previously stated, hydrogen bonding can play a very important role in conformational preferences of peptidomimetics. On the one hand, intramolecular hydrogen bonds can stabilize a given geometry, and on the other hand, the H-bonding pattern with the solvent is essential for the solvation of a molecule. Thus, H-bonding could affect both entropy and enthalpy of a determined structure in solution. Probably one of the most useful parameters for that study is the temperature dependence of amide N*H* chemical shift ($\Delta\delta$N$H/\Delta T$). The temperature factors of **1a,b** and **2a,b** are given in Table 3, measured in both the solvent and the temperature range of the VT-NMR experiments.

Considering the classification done by Gennari and Scolastico,[19] the temperature factors for the small cyclophanes **1a,b** (entries 1 and 3 in Table 3) would correspond to an equilibrium between intramolecular H-bonded and solvent exposed amide N*H* protons. This is in agreement with the high polarity and H-bonding ability of DMSO. Thus, even in this very polar solvent, the intramolecularly H-bound species are important for these macrocycles. On the other hand, the values obtained for the larger cyclic structures (entries 2 and 4 in Table 3) would agree with strong intramolecular hydrogen bonds concerning amide NH protons. Moreover, the smaller value for **2b** compared to that of **2a** suggests that the hydrogen bonding pattern is somehow stronger with R = Bn than with R = ^{i}Pr. This could give us a clue for the enthalpic difference in the energy barrier observed for **2a**/**2b**. The more favored H-bound species would stabilize the GS and therefore increase the $\Delta H^{\ddagger}$ value. From all these data, we can conclude that the intramolecular H-bonds play an important role in the conformational movement and have to be considered for further discussions.

(17) All line shape simulations were performed using the gNMR V4.1.0 program, provided by Cherwell Scientific, Oxford, Great Britian.

(18) This entropic contribution has been previously reported in related systems: (a) Chang, M. H.; Masek, B. B.; Dougherty, D. A. *J. Am. Chem. Soc.* **1985**, *107*, 1124−1133. (b) Chang, M. H.; Dougherty, D. A. *J. Am. Chem. Soc.* **1983**, *105*, 4102−4103.

(19) (a) Alonso, E.; López-Ortiz, F.; Del Pozo, C.; Peralta, E.; Macías, A.; González, J. *J. Org. Chem.* **2001**, *66*, 6333−6338. (b) Belvisi, L.; Gennari, C.; Mielgo, A.; Potenza, D.; Scolastico, C. *Eur. J. Org. Chem.* **1999**, 389−400.

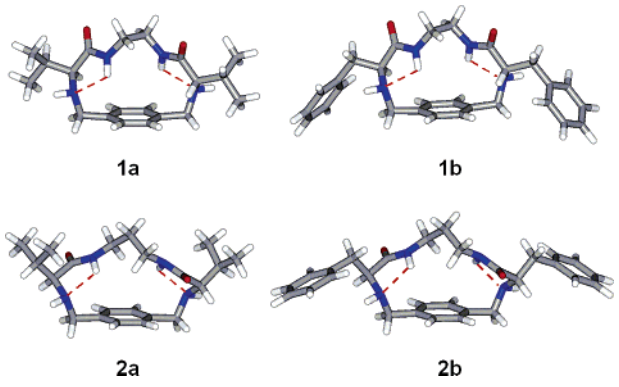

FIGURE 4. Minima of energy for compounds **1a,b**−**2a,b**. Hydrogen-bonding interactions are highlighted as red dashed lines.

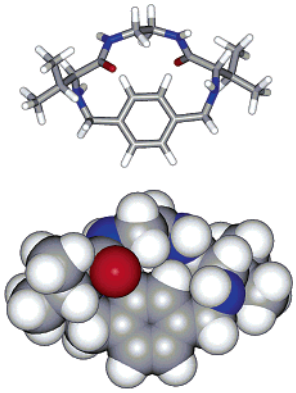

FIGURE 5. Semiempirical (AM1) optimized geometry found for the TS of **1a** in stick (top) and space filling (bottom) representations.

Molecular Modeling. To get a clearer picture of the more stable conformations of these peptidomimetic cyclophanes, a Monte Carlo random conformational search with MMFF94 force field minimization was performed for every compound.[20] The global minima of energy thus obtained for every macrocycle are shown in Figure 4.

All of them showed the *p*-diphenylene moiety perpendicular to the macrocyclic main plane, in good agreement with the reported crystal structure of **1a**.[13] This disposition would set the peptidomimetic arm on top of the anisotropy cone of the aromatic ring, explaining the observed upfield shift of the corresponding signals, which is specially important for the amide N*H* protons. Amide protons are H-bonded to the amino nitrogens, forming five-membered rings. This forces the amide N*H* to point to the inner cavity of the macrocyclic compound, this effect being specially dramatic for the smaller 16-membered ring systems **1a,b**. Space filling views of these minima showed that in the cases of **1a,b** amide protons would almost completely fill the macrocyclic cavity. For the conformational process depicted in Scheme 1, the rotation of the aromatic ring would be disfavored by this disposition of amide N*H* fragments. To illustrate this, the TS of **1a** for this conformational process has been also optimized and is shown in Figure 5.

Again the CPK model of this TS (Figure 5, bottom) showed how the macrocyclic cavity is completely filled, in this case by the −CH═CH− fragment of the *p*-diphenylene moiety. The amide NH's are now almost perpendicular to the macrocycle and pointing to opposite faces of the molecule. This arrangement would make it impossible to establish the H-bonding pattern found for the conformation of minimum energy, and thus the rotation of the aromatic ring with respect to the macrocycle will imply the breaking of the intramolecular H-bonding pattern. Additionally, the disposition of amide groups in the TS will favor their solvation, which would be precluded in the GS, as they are pointing to the inner cavity of the molecule. Then, with this model, we can explain the higher solvation of the TS with respect to the GS, which would account for a negative contribution to $\Delta S^{\ddagger}$. At the same time, the TS is itself more rigid than the GS and thus more ordered, also contributing to a negative $\Delta S^{\ddagger}$. Regarding the larger cycles **2a,b**, the effect of molecular constriction would be less pronounced as the larger size of the cavity will relax, at least in some extent, the strain energy in TS.

Inspection of the 10 lowest energy conformers for every compound, which are located within an energy gap of 3 kcal/mol, showed that the peptidomimetic moiety is a bit more flexible for **2a,b** than for **1a,b**, as expected for the different ring size (see Supporting Information). Besides, these structures suggested a rather free movement of the side chains for all of the compounds. In the case of **1b** and **2b**, this movement would dramatically increase the steric hindrance close to the amino group. The average spatial proximity of the aromatic side chain to the *p*-diphenylene fragment is supported by the upfield shift suffered by both benzylic and aromatic protons of this moiety (see Supporting Information), compared with **1a** and **2a**, respectively.

According to this scenario, the presence of the benzyl residues would make the amino groups less accessible to the solvent molecules. As these groups are directly implicated in the hydrogen-bonding pattern, the aromatic side chain would protect the hydrogen bond from the solvent. This effect would account for a lower solvation in the GS for **1b** than for **1a**, as in DMSO these compounds have their amide N*H* protons partially solvent exposed (as demonstrated from temperature factors). For **2a,b**, the situation in chloroform is quite different as they exist as intramolecularly H-bonded species. Then, the hydrogen bonds are strong in the conformations of the GS and must be partially broken to reach the TS. Once again, the presence of the benzyl group would protect these H-bonds from the influence of the solvent, making the GS of **2b** enthalpically more stable than that for **2a** (relative to the corresponding TS's). This observation also agrees with the lower $\Delta\delta$N*H*/ΔT value of **2b** with respect to **2a**. Then, the effect of the intramolecular hydrogen bond on the conformational stability clearly depends on the bulk solvent, as discussed below.

Effect of Solvent on the Conformational Stability. Taking into account the former discussions, all data obtained point out the fact that there is a direct relationship between the conformational process and the ability of forming intramolecular hydrogen bonds. Thus, the stronger and more probable those H-bonds, the higher is the energy barrier for the rotation of the aromatic ring. Intramolecular H-bonds will be less favorable in polar solvents, as solvent molecules would effectively compete. Thus, the free energies of activation for the ring inversion of a given peptidomimetic cyclophane would be lower in a polar solvent, able to form H-bonds with the amide groups, than in a nonpolar environment. This idea is depicted in Scheme 2.

The interaction of a polar solvent with the amide groups would break the intramolecular hydrogen bonds, opening the

(20) All molecular modeling was performed using Spartan Pro, version 1.0.5, provided by Wavefunction, Inc., Irvine, CA.

SCHEME 2. Effect of Polar Solvents on the Conformational Stability of Peptidomimetic Macrocyclic *p*-Cyclophanes[a]

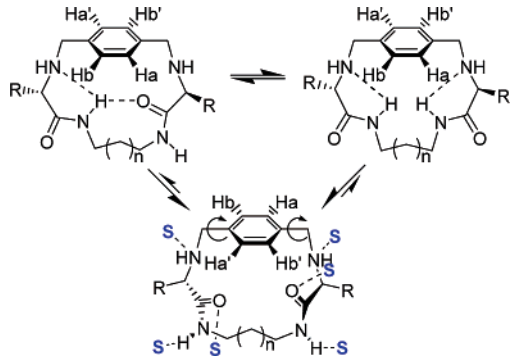

[a] The interaction of the peptidomimetic moiety with a polar and H-bonding solvent (depicted as blue S) would open the macrocyclic cavity, increasing the rate of the rotation of the aromatic *p*-diphenylene fragment.

TABLE 4. VT-NMR Data for 1a,b−2a,b in Different Solvents

entry	compound	$\delta\nu$[a]	T_c (K)	$\Delta G^{\ddagger}_c$ (kcal/mol)[b,c]	solvent
1	**1a**	34.0	>413[d]	>20.9[e]	TCE[f]
2	**2a**	130.8	240	11.3	acetone-d_6[g]
3	**1b**	30.5	>413[d]	>20.9[e]	TCE[f]
4	**2b**	146.8	260	12.2	acetone-d_6[g]

[a] Measured at the low-temperature spectra. [b] Calculated using the approximated formula for temperature of coalescence and considering the coupling constant between interconverting protons (J_{AB}). [c] Estimated error ±0.4 kcal/mol. [d] Coalescence not observed. [e] Estimated. [f] TCE: 1,1,2,2-tetrachloroethane-d_2. [g] Because of solubility problems, a 10% of CD_3OD was added.

macrocyclic cavity and increasing the solvation of the GS conformations. This additional interaction with solvent molecules would compensate the energy cost upon intramolecular H-bonds breaking. The expected effect would be an acceleration of the aromatic ring rotation. To check our proposal, we repeated the VT-NMR experiments but using a less polar solvent for **1a,b** (deuterated 1,1,2,2-tetrachloroethane, TCE) and a very polar environment for **2a,b** (a 9:1 mixture of CD_3COCD_3/CD_3OD), and the results are shown in Table 4. The results nicely support our initial hypothesis. Thus, heating the sample of either **1a** or **1b** in a solvent more hydrophobic than DMSO, such as TCE, only produced a smooth broadening of the AA′BB′ signal, with no signs of coalescence within the accessible temperature range. This implies that a nonpolar environment clearly stabilizes the conformation in the GS and destabilizes the TS as solvation is less efficient, with a final effect of a higher rotational energy barrier. Moreover, temperature factors of the amide chemical shifts ($\Delta\delta NH/\Delta T$) of these compounds in TCE were also measured, being −3.56 ppb/K for **1a** and −2.51 ppb/K for **1b**. Once again, these data support the fact that the intramolecular hydrogen bonds are more stable for the macrocycle with benzyl side chains. Unfortunately, the high stability of the GS conformations in this solvent made it impossible to extract more quantitative information about the thermodynamic activation parameters. Despite that, the impressive increase of the conformational stability of **1a,b** when using a less polar environment is remarkable.

Regarding the 17-membered ring systems, data in Table 4 also support our initial proposal. For instance, the temperature of coalescence of **2a,b** decreased ca. 60 K when increasing the polarity and the H-bonding ability of the solvent (compare

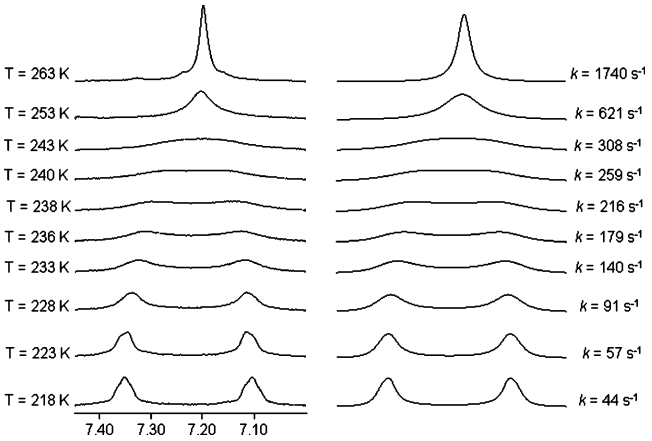

FIGURE 6. Aromatic *p*-diphenylene region of the experimental (left) and simulated (right) VT-NMR spectra of **2a** (5 mM, 9:1 CD_3COCD_3/CD_3OD, 500 MHz). Values of temperature (T, K) and interconversion rate (k, s^{-1}) are also given for every trace. Simulated spectra were obtained with the gNMR program.[17]

entries 2 and 4 in Table 4 with entries 2 and 5 in Table 1, respectively). Accordingly, the $\Delta G^{\ddagger}$ at T_c decreased about 3 kcal/mol, supporting the lower energy barrier for the rotation of the aromatic ring of these systems in polar environments. Unfortunately, a high degree of overlapping signals for **2b** precluded the accurate simulation of its spectra at different temperatures, while line shape analyses were possible in the case of **2a** (Figure 6).

Thus, ln(k) versus 1/T gave a value of Arrhenius activation energy of E_a = 8.8 kcal/mol, 2 kcal/mol lower than the one measured in chloroform. More informative data were obtained from the Eyring plot, which rendered $\Delta H^{\ddagger}$ = 8.3 kcal/mol, $\Delta S^{\ddagger}$ = −12.4 cal/K/mol and $\Delta G^{\ddagger}_{(298\ K)}$ = 11.2 kcal/mol. If we compare these data with those obtained in chloroform (entry 2 in Table 2) once again, a lower free energy of activation ($\Delta\Delta G^{\ddagger}_{(298K)}$ = 3.3 kcal/mol) was obtained in a polar solvent. Regarding the different enthalpic and entropic contributions to the free energy of activation, both are affected by the solvent polarity. The difference in the enthalpy of activation ($\Delta\Delta H^{\ddagger}$ = 1.9 kcal/mol) reflects the breaking of intramolecular H-bonds in the GS conformations by interaction with the solvent, leading to an enthalpic destabilization of the GS. Besides, the entropic contribution also decreased ($\Delta\Delta S^{\ddagger}$ = 2.0 cal/K/mol), suggesting that the molecular order of the GS is somewhat higher in polar solvents, because the hydrogen bonds would order more solvent molecules around the macrocycle. Thus, polar solvents would weaken intramolecular H-bonds and would efficiently solvate both the GS and TS conformations. The overall effect is an acceleration of the rotation of the aromatic ring and thus a more dynamic system in solution. An extrapolation of these results would explain the differences obtained for R = ^{i}Pr and R = Bn. The higher rigidity of the aromatic derivatives can be also understood by the higher stability and/or probability of the intramolecular H-bonds and the presence of less solvated structures in the GS of these derivatives. This proposal agrees both with the dynamic NMR study and the temperature factors of NH chemical shifts. It is also illustrated by molecular modeling, where the movement of the side chain in the minima of compounds **1b**,**2b** would partially shield the benzylic amino nitrogen from interaction with solvent molecules. All these ideas are schematically depicted in Figure 7.

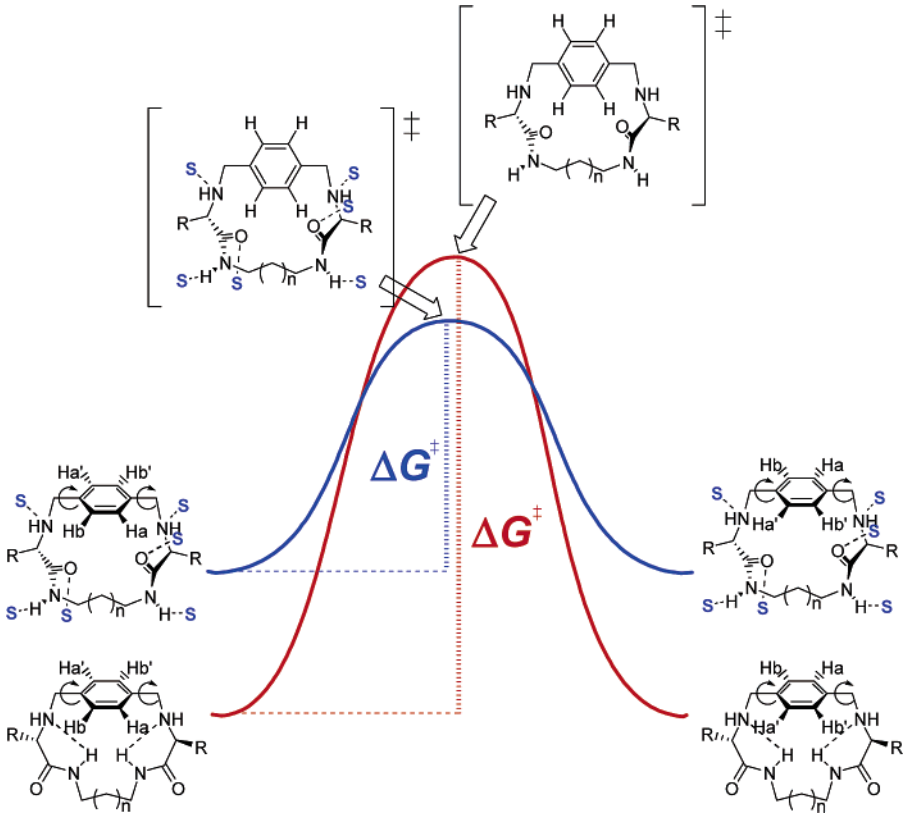

FIGURE 7. Schematic representation of the proposed mechanism for the effect of polar solvents on the energy barrier of the inversion of the peptidomimetic cyclophanes. The polar solvent would break the intramolecular H-bonds in the GS and solvate more efficiently both the GS and the TS.

Methanol-Fueled Artificial Molecular Rotor: Intramolecular H-bonding as a Molecular Brake. The observation of the conformational behavior of **1a,b**−**2a,b** in different environments encouraged us to set an experiment, playing with the relationship between H-bonding pattern and rate of rotation of the aromatic ring. Thus, by selecting the right combination of ring size, side-chain and solvent mixtures, we were able to develop a system behaving as an artificial molecular rotor at room temperature. A very graphical example was obtained in the case of compound **2b** (n = 1, R = Bn) in $CDCl_3$. In this specific case, this minimalistic molecular device, in which the aromatic moiety can rotate with respect to the macrocyclic main ring, is able to nicely respond to external stimuli. Results shown in Figure 8 clearly demonstrate that the rate of rotation of the *p*-diphenylene moiety is dependent on the concentration of MeOH. When acquiring the ^{1}H NMR spectrum of **2b** (500 MHz, 303 K, $CDCl_3$) the signals for protons of diphenylene moiety formed a broad AA′BB′ spin system at an interconversion rate of about 40 s^{-1}. When known amounts of MeOH were added, the above-mentioned signals started to broaden more until reaching coalescence at 5% MeOH. Concomitantly, amide N*H* signals moved downfield as an effect of the formation of intermolecular H-bonds with the molecules of solvent and a conformational movement as depicted in Figure 7. This scenario implies a nearly 3-fold acceleration of the rate of the phenylene rotation due to the presence of only 5% MeOH. Additionally, the reversibility of the process has been also shown. Then, when MeOH molecules were withdrawn from the medium (by using freshly activated 4 Å molecular sieves) the macrocycle recovered its conformational rigidity, reflected in the anisochronic aromatic

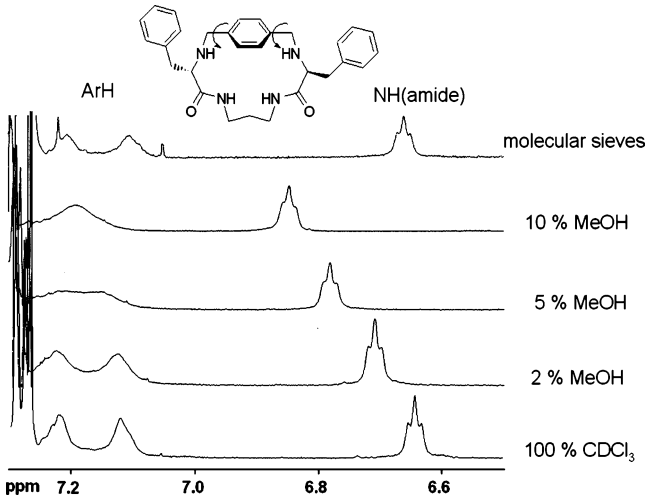

FIGURE 8. Methanol-dependent conformational movement of **2b**.

p-diphenylene signals (Ar*H*), as well as in the recovering of the original amide protons chemical shift (see upper trace in Figure 8).

These observations clearly demonstrate the relationship between H-bonding, solvent accessibility, and conformational stability of our peptidomimetic systems. In this simple device, the rotation at the molecular level is accelerated by methanol molecules. The effect of this external stimulation produces enough energy to break the intramolecular H-bonding, by forming intermolecular ones with the solvent. Otherwise, in the absence of this molecular *fuel*, intramolecular H-bonds behave

as an internal *brake* for the aromatic moiety rotation. Considering this model and the VT-NMR measurements performed in solvents with different polarities, we attempted to estimate the energy for the acceleration produced by the external fuel as well as the brake strength. Considering that in the free rotation regime at room temperature the measured energy barrier is ca. 3 kcal/mol lower than in a nonpolar environment, we propose the energy provided by our external fuel to be of that order. Interestingly, this value would correspond to the energy of two favored (intramolecular) hydrogen bonds,[21] which nicely fit our modeling studies. Thus, the braking strength in our molecular rotor nicely correlates with the difference in the rotational barrier of the dynamic process when decreasing the polarity of the solvent, namely the energy for the observed deceleration. The deep understanding of this specific molecular motion opens the way for the design of more elaborated devices, able to show an externally controlled movement. With this study and considering the modularity and easy syntheses of our systems, we have the tools for the development of more sophisticated molecular machines.

Conclusions

A complete conformational analysis of different peptidomimetic macrocyclic cyclophanes has been carried out with the help of VT-NMR and molecular modeling techniques. The rotation rate of the aromatic ring of the *p*-diphenylene moiety occurs within the NMR time scale range, which has allowed us to deeply study this dynamic process. From the VT-NMR experiments, clear tendencies have been observed that depend on the macrocyclic ring size and the nature of the side chain of the peptidomimetic fragment. Values of thermodynamic activation parameters have been obtained in most of the examples, leading to a different enthalpic/entropic contribution to the free energy of activation of the macrocyclic ring inversion. Of note are the negative values of $\Delta S^{\ddagger}$, which can be due to a large molecular constriction and/or higher solvation of the TS, as compared with the GS. The participation of the intramolecular hydrogen-bonding pattern in the GS has also been evidenced by the measurement of temperature factors of amide N*H* chemical shifts. These intramolecular H-bonds have been characterized with the help of molecular modeling. Semiempirical theoretical quantum mechanics calculations on the TS also suggested the importance of the disposition of the amide NH bonds for the rotation of the *p*-diphenylene moiety. There is a clear relationship between the intramolecular H-bonds and the conformational flexibility of the systems: the more stable the intramolecular H-bonds, the slower the conformational process. Thus, there must be a competition between the rotation of the ring and the establishment of intramolecular H-bonds. Studies with solvents of different polarities supported this hypothesis. Both the effect of the nonpolar solvents and that of the benzyl side chains can be understood in terms of the ability of the system to create a microenvironment in which intramolecular H-bonds are more stable and probable, with a lesser competition from hydrogen bonding to the solvent. This solvent dependence of conformational stability is a very interesting topic, in close relationship with enzymatic activity and protein folding processes. We believe that our peptidomimetic systems could serve as very simple models for the study of the relationship between environment and conformation of more complicated biomolecules. Also, their conformational preferences would be crucial when using our systems in molecular recognition, catalysis or sensing events, as well as for the design of new molecular devices. As a matter of fact, we were able to show how one of our compounds behaves as a minimalistic artificial molecular rotor, dependent on the presence of an external stimuli. A very simple experiment demonstrated how intramolecular hydrogen bonds can act as a remote molecular brake and the added methanol molecules as the fuel to provide the system with enough energy to overcome the braking strength, accelerating the molecular rotation. By withdrawing the fuel from the medium, the brakes are restored and the rotation of the aromatic ring slowed back to the initial rate. This study leads to the understanding of this molecular movement, which would be of great importance for future applications of these and other related systems in supramolecular chemistry.

Experimental Section

Compounds **1a,b**−**3a,b** were synthesized as previously described and showed the expected spectroscopic and analytical data.[13] Samples were prepared by weighing the necessary amount of peptidomimetic cyclophane and adding a known volume (typically 0.7 mL) of the desired deuterated solvent. The final concentration was 5−10 mM in all cases. To take advantage of the magnetic field value, measurements requiring temperatures higher than room temperature for observing coalescence were performed in an apparatus with a proton resonance frequency of 300 MHz. Conversely, when cooling was necessary to achieve decoalescence, a 500 MHz (also for ^{1}H NMR) magnetic field was used. The temperature of each NMR spectrometer was calibrated by the methanol method in separate experiments.[22] The accuracy in temperature measurement was at least ±1 K. The reversibility of the changes produced in NMR signals was checked by repeated measuring at different temperatures. The approximated values of the free energy of activation ($\Delta G^{\ddagger}_c$) at the coalescence temperature (T_c) were obtained from the following formula: $\Delta G^{\ddagger}=RT_c[22.96 + \ln\{T_c/[(\nu_A - \nu_B)^2 + 6J_{AB}^2]^{1/2}\}]$.[16] Fitting of dynamic NMR line shapes at different temperatures were performed with the gNMR program.[17] The activation parameters were calculated by the least-squares fitting of suitable plots of the corresponding kinetic values obtained from the line-shape analysis and the measured temperatures of the experimental spectra (Supporting Information). As the simulation could be carried out at several temperatures (eight or more), the estimated error in $\Delta G^{\ddagger}$ is about ±0.15 kcal/mol.[23] For the molecular modeling studies, a PC version of Spartan Pro program was used.[20] To obtain the minima of energy on the GS, the *conformer distribution calculation* option available in Spartan Pro was used.[20] With this option, an exhaustive Monte Carlo search without constraints was performed for every structure. The torsion angles were randomly varied, and the obtained structures were fully optimized using the MMFF94 force field. Thus, 100 minima of energy within an energy gap of 10 kcal/mol were generated. These structures were analyzed and ordered considering the relative energy, the repeated geometries being eliminated. For the TS of **1a**, the *transition state optimization* option available in Spartan Pro was used, the geometry being fully optimized at the semiempirical AM1 level of theory. Frequencies calculation showed that the geometry is a real transition state, showing an imaginary frequency. The vibrational modes were computed, and the eigenmode corresponding to the negative eigenvalue was generated and visually inspected with the animation facility implemented in Spartan Pro.

(21) Williams, D. H.; Stephens, E.; O'Brien, D. P.; Zhou, M. *Angew. Chem., Int. Ed.* **2004**, *43*, 6596−6616.

(22) Braun, S.; Kalinowski, H.-O.; Berger, S. *150 and More Basic NMR Experiments*; Wiley-VCH: Weinheim, 1988.

(23) Bonini, B. F.; Grossi, L.; Lunazzi, L. *J. Org. Chem.* **1986**, *51*, 517−522.

Acknowledgment. Financial support from the Spanish Ministerio de Ciencia y Tecnología (BQU2003-09215-C03-02) Bancaixa-UJI (P1B2004-38) and Generalitat Valenciana (GRUPOS 04/031) is gratefully acknowledged. I.A. thanks MEC for personal financial support (Ramón y Cajal Program).

Supporting Information Available: $^{1}H-^{1}H$ COSY spectra of **1a,b**−**3a,b** compounds, experimental and simulated partial NMR spectra at different temperatures, Arrhenius and Eyring plots, plots of δNH (ppm) vs T (K), superimposed 10 lowest energy minima and selected NMR chemical shift in different solvents for **1a,b**−**2a,b**, Cartesian coordinates for the obtained minima of **1a,b**−**2**,**a,b** and for the transition state of **1a**. This material is available free of charge via the Internet at http://pubs.acs.org.

JO051974I